Volume XCIV, No. 1, May 2024

Proceedings of the Danish Society for Structural Science and Engineering

Published by

Danish Society for Structural Science and Engineering

COPENHAGEN 2024

ISSN 1601-6548 (online)

PROCEEDINGS OF THE DANISH SOCIETY FOR STRUCTURAL SCIENCE AND ENGINEERING
Edited and published by the Danish Society for Structural Science and Engineering
Volume 94, No. 1, 2024.

Section force distribution in a square foundation affected by a centrally located point load

Lars German Hagsten[1]

Introduction

This article presents a lower bound solution for a square foundation subjected to a centrally located point load. The analysis begins by considering a square foundation subjected by a load concentrated at a single point. Then, the investigation extends to cases where the load is distributed over a finite area, incorporating the specific conditions that arise in such scenarios.

The primary objective of this article is to explore the similarities and differences in the distribution of section forces between square and circular foundations. While the distribution of section forces in circular foundations has been addressed in previous studies [1], [2], this work focuses on square foundations. Key aspects under investigation include the relationship between the maximum moment in circular and square foundations and the variation of tensile forces in the reinforcement near the edge. Similar to the approach used for circular foundations, the analysis assumes isotropic, orthogonal reinforcement and that the foundation is supported by an evenly distributed reaction.

The study first examines the square foundation under a concentrated point load, followed by an analysis of the implications of a load distributed over a finite area.

Square foundation affected by a point load acting in a single point

A square point foundation with side length $2a$ is considered. The foundation is affected by a centrally located point load, P, and supported by a uniformly distributed reaction, p, see Figure 1.

[1] Aarhus University, Value Engineering ApS

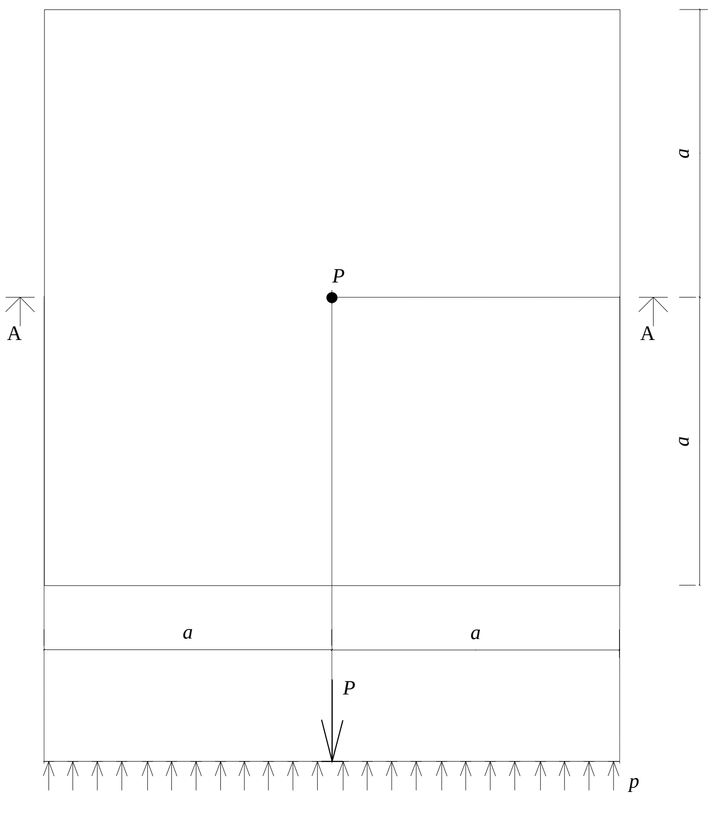

Figure 1 Square point foundation acted upon by a centrally located point load and supported by a uniformly distributed reaction

The description of the distribution of the section forces in the plate is generally divided into two sub-investigations. The known solution for a circular foundation [1] is used to describe the distribution of the section forces of the part of the reaction that acts within the largest circle that can be placed in the square, see figure 2, where it thus applies that $a = R$.

Since $a = R$, the moment distribution corresponding to this part of the reaction and within the circle is given by:

$$m_{r,c}(r) = 0 \quad (1)$$

$$m_{\theta,c} = \frac{P}{2\pi}\left(1 - \left(\frac{r}{a}\right)^2\right) \quad (2)$$

With $P = P_c = \pi a^2 \cdot p$ since only the part located inside the circle is considered, (2) can be rewritten to:

$$m_{\theta,c} = \frac{1}{2}\left(1 - \left(\frac{r}{a}\right)^2\right) a^2 \cdot p \quad (3)$$

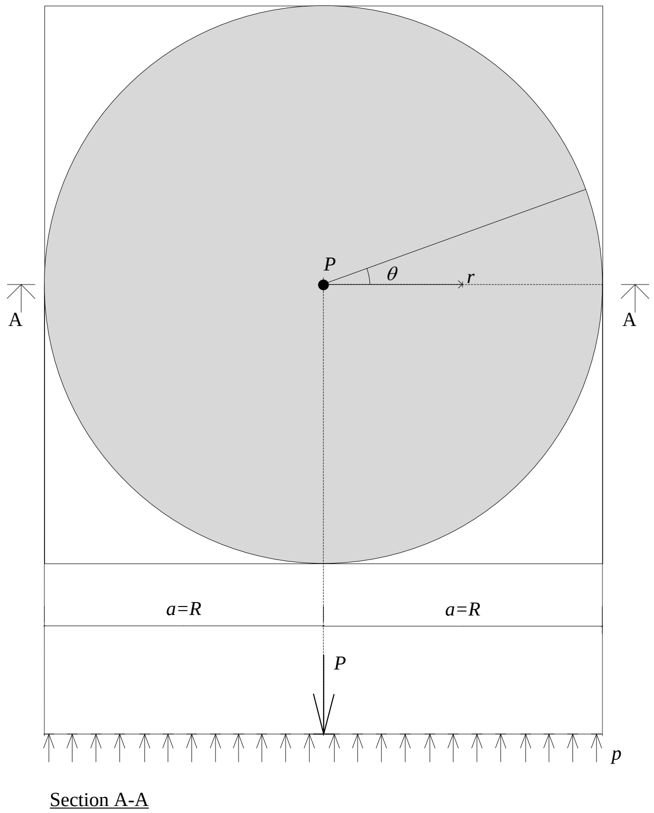

Figure 2 Part of reaction acting within the largest circle that can be placed in the square highlighted

To these moments are added the moments originating from the part of the reaction which is located outside the circle, see figure 3.

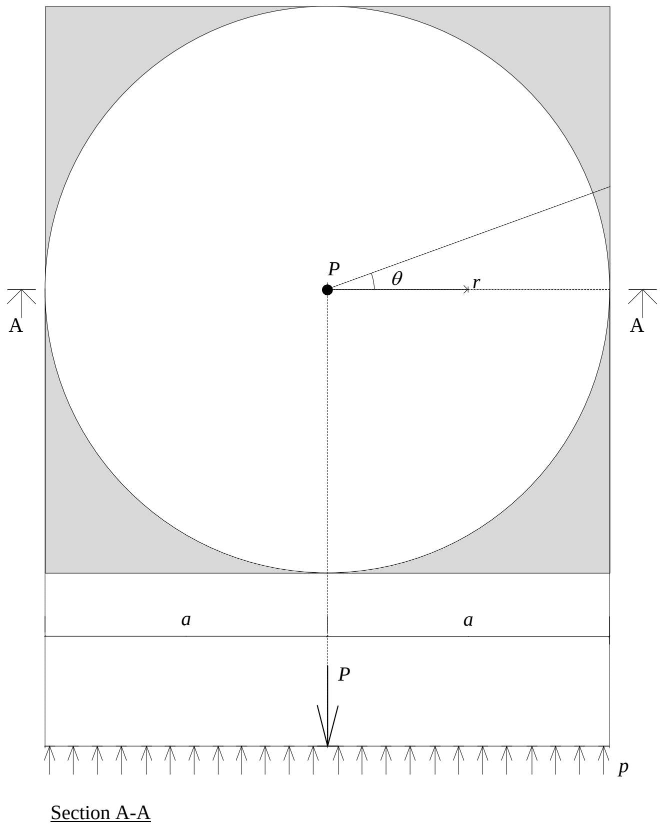

Figure 3 Part of reaction acting outside the largest circle that can be placed in the square highlighted

This part of the load is initially carried to the periphery of the circle.

In the following, three models are described for how this part of the reaction can be carried to the periphery of the circle. Due to uniform conditions is seen only in the range of $\theta \in [0; \frac{\pi}{4}]$.

Model 1

The reaction acting below the shaded areas in figure 3 is carried to the periphery of the circle via fan-shaped strips. The fans are delimited by radians. This model is illustrated in Figure 4.

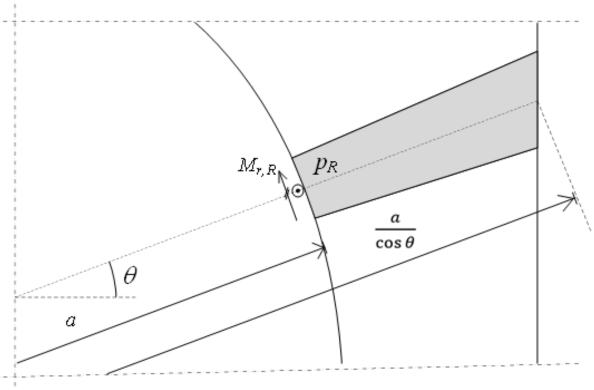

Figure 4 Model 1. Illustration of applied fan-shaped strips

By bringing the reaction to the periphery in this way, there is a line load/reaction, p_R, and moment on the edge ($m_{r,R}$ ($a = R$) given by:

$$p_R = \left(\frac{1}{2 \cdot \cos^2\theta} - \frac{1}{2}\right) a \cdot p \tag{4}$$

$$m_{r,R} = \frac{1}{6}\left(\frac{1}{\cos\theta} - 1\right)^2 \left(1 + \frac{2}{\cos\theta}\right) a^2 \cdot p \tag{5}$$

Figure 5 shows the variation of $p_R(\theta)$ and $m_R(\theta)$ along the circumference of the inscribed circle.

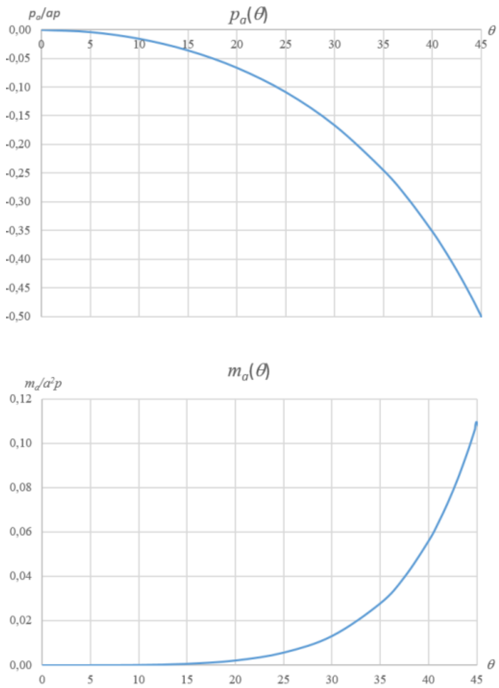

Figure 5 Model 1. $p_R(\theta)$ and $m_R(\theta)$

Model 2

Model 2 and model 3 both make use of the fact that the reaction is carried to the circle periphery by strips parallel to the *x* and *y* axis respectively. Both strips are modeled as cantilevered strips supported/clamped along the circle. All sub-areas in the shaded areas are thus covered by a strip in both directions.

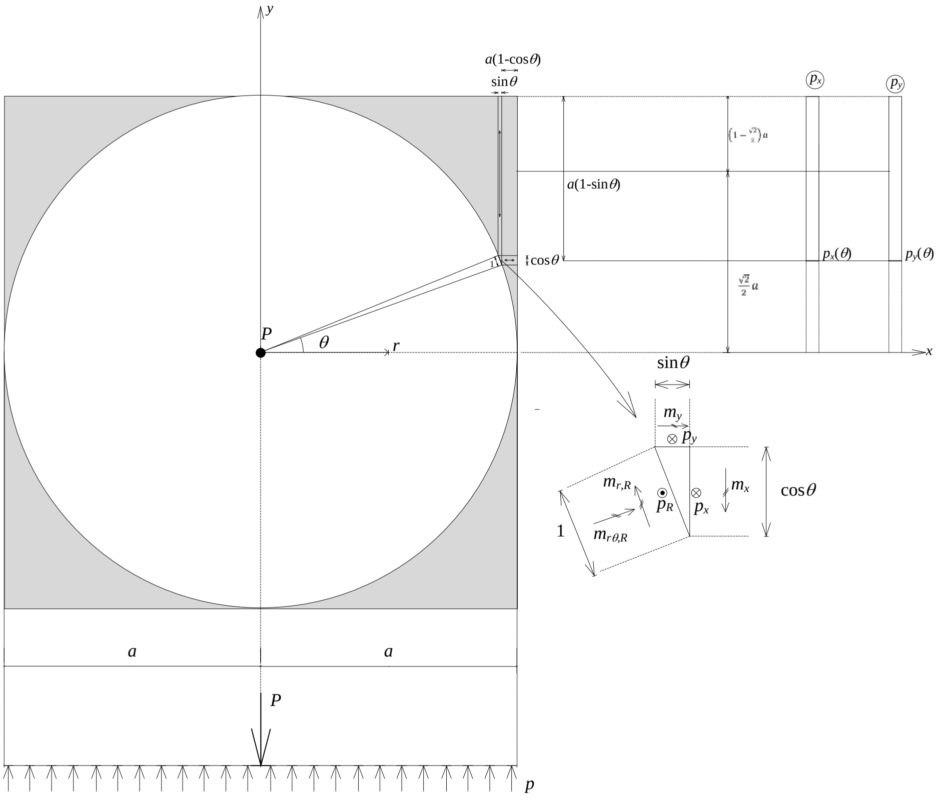

Section A-A

Figure 6 Model 2. Reaction is carried to the circle periphery by strips parallel to the x and y axis. Constant p_x and p_y

A small section of the circle with length "1" is considered, see Figure 6. At the circle, each of the two strips delivers a reaction, respectively p_x and p_y, as well as a moment, respectively m_x and m_y. Along the circle it gives the reactions $m_{r,R}$, $m_{r\theta,R}$ and p_R. These are determined for $\theta \in \left[0; \frac{\pi}{4}\right]$ by:

$$m_{r,R} = m_x \cos^2\theta + m_y \sin^2\theta \tag{6}$$

$$m_{r\theta,R} = m_x \cos\theta \sin\theta - m_y \sin\theta \cos\theta \tag{7}$$

$$p_R = p_{x,a} \cos\theta + p_{y,a} \sin\theta \tag{8}$$

The simplest possible way to distribute the reaction is for the individual strips to be affected by half of the evenly distributed reaction, that is $p_x = p_y = -½p$. This is done in model 2.

$$p_{x,a} = -(½p)a(1-\cos\theta) \tag{9}$$

$$p_{y,a} = -(½p)a(1-\sin\theta) \tag{10}$$

$$m_x = \frac{1}{2}(½p)a^2(1-\cos\theta)^2 \tag{11}$$

$$m_y = \frac{1}{2}(½p)a^2(1-\sin\theta)^2 \tag{12}$$

With the expressions for p_x ,p_y, m_x og m_y inserted:

$$m_{r,R} = \frac{1}{4}pa^2(1-\cos\theta)^2 \cos\theta \sin\theta + \frac{1}{4}pa^2(1-\sin\theta)^2 \sin\theta \cos\theta \tag{13}$$

$$m_{r\theta,R} = \frac{1}{4}pa^2(1-\cos\theta)^2\cos\theta\sin\theta - \frac{1}{4}pa^2(1-\sin\theta)^2\sin\theta\cos\theta \quad (14)$$

$$p_R = \frac{1}{2}pa(1-\cos\theta)\cos\theta + \frac{1}{2}pa(1-\sin\theta)\sin\theta \quad (15)$$

p_R, $m_{r,R}$ and $m_{r\theta,R}$ are shown in figure 7.

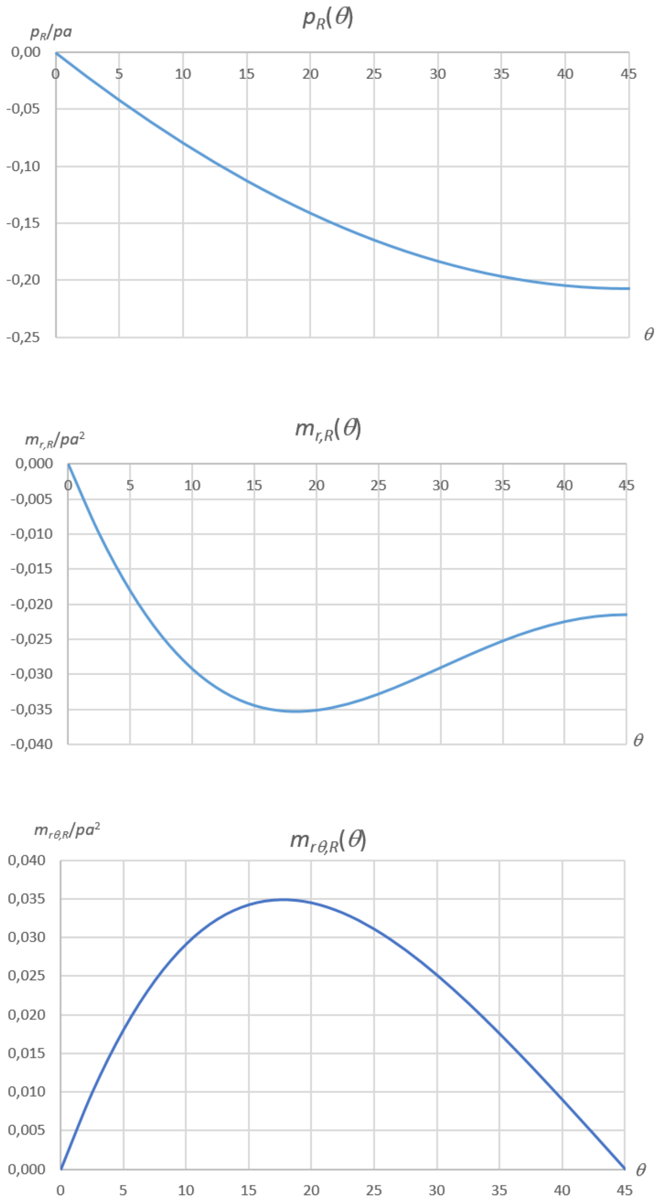

Figure 7 Model 2. $p_R(\theta)$, $m_R(\theta)$ and $m_{r\theta,R}$

Model 3

In the darkest shaded areas in the corners of the foundation, see Figure 8, it is assumed that the reaction is distributed equally in the *x* and *y* directions, i.e. $p_y = p_x = -½p$. In what follows, the area considered is limited by $0 \le y \le x$ and $0 \le x \le a$. That part corresponds to one-eighth of the foundation, and the other parts are the same (half of them mirrored).

No section forces are transferred between the eight identical sub-areas. This is utilized when determining the distribution of the reactions in the two directions. Look at a strip on the outer (for $x = a$) haves for $y \in [0; \frac{\sqrt{2}}{2}a]$, if it is required that p_y is a continuous function and the resulting reaction must be 0, then p_y can be expressed by:

$$p_y = \left(\frac{1}{2} - \sqrt{2} + 2y\right)p \tag{16}$$

This is considered valid throughout the considered area (the light shaded area), and thus constant in the x direction.

p_x is given by:

$$p_x = p - p_y \tag{17}$$

i.e for $y \in [0; \frac{\sqrt{2}}{2}a]$:

$$p_x = \left(\frac{1}{2} + \sqrt{2} - 2y\right)p \tag{18}$$

p_x og p_y are illustrated in figure 8.

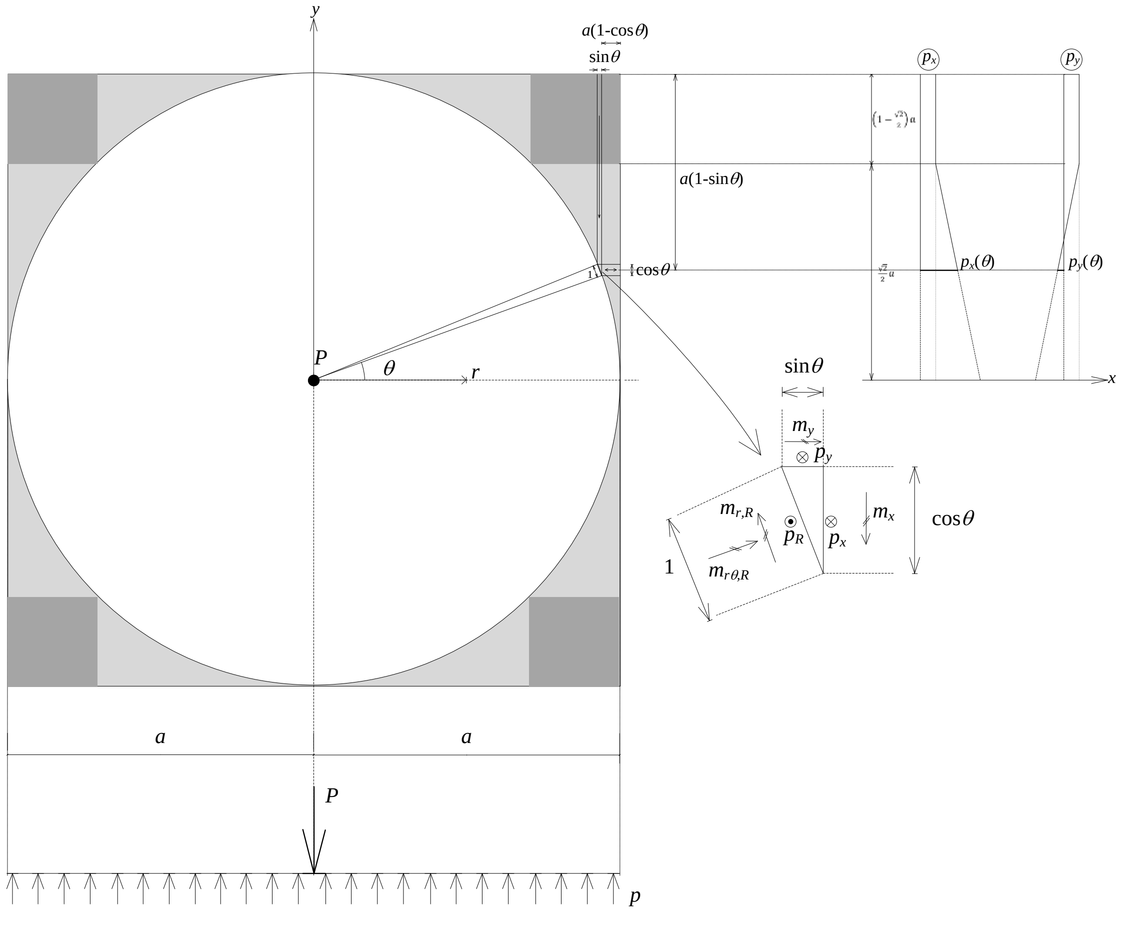

Figure 8 Model 3. Reaction is carried to the circle periphery by strips parallel to the x and y axis. Varying p_x and p_y

From the expressions for p_x and p_y follows:

$$v_x = \left(\frac{1}{2} + \sqrt{2} - 2\frac{y}{a}\right)\left(\frac{x}{a} - 1\right)ap \quad \text{for } y \in [0; \frac{\sqrt{2}}{2}a] \tag{19}$$

$$v_y = \left(\left(\frac{1}{2} - \sqrt{2}\right)\frac{y}{a} + \left(\frac{y}{a}\right)^2\right)ap \quad \text{for } y \in [0; \frac{\sqrt{2}}{2}a] \tag{20}$$

$$m_x = \frac{1}{2}\left(\frac{1}{2} + \sqrt{2} - \frac{2y}{a}\right)\left(1 - \frac{x}{a}\right)^2 \cdot a^2 p \qquad \text{for } y \in [0; \tfrac{\sqrt{2}}{2}a] \qquad (21)$$

$$m_y = \left(\frac{1}{4}\left(1 - \frac{\sqrt{2}}{3}\right) + \frac{1}{2}\left(\frac{1}{2} - \sqrt{2}\right)\left(\frac{y}{a}\right)^2 + \frac{1}{3}\left(\frac{y}{a}\right)^3\right) a^2 p \qquad \text{for } y \in [0; \tfrac{\sqrt{2}}{2}a] \qquad (22)$$

Since $\frac{x}{a} = \sqrt{1 - \left(\frac{y}{a}\right)^2}$ and $\frac{y}{a} = \sin\theta$ the section forces along the periphery of the inscribed circle can be expressed by α and θ:

$$v_x = \left(\frac{1}{2} + \sqrt{2} - 2\sin\theta\right)\left(\sqrt{1 - (\sin\theta)^2} - 1\right) ap \qquad \text{for } y \in [0; \tfrac{\sqrt{2}}{2}a] \qquad (23)$$

$$v_y = \left(\left(\frac{1}{2} - \sqrt{2}\right)\sin\theta + (\sin\theta)^2\right) ap \qquad \text{for } y \in [0; \tfrac{\sqrt{2}}{2}a] \qquad (24)$$

$$m_x = \frac{1}{2}\left(\frac{1}{2} + \sqrt{2} - 2\sin\theta\right)\left(1 - \sqrt{1 - (\sin\theta)^2}\right)^2 \cdot a^2 p \qquad \text{for } y \in [0; \tfrac{\sqrt{2}}{2}a] \qquad (25)$$

$$m_y = \left(\frac{1}{4}\left(1 - \frac{\sqrt{2}}{3}\right) + \frac{1}{2}\left(\frac{1}{2} - \sqrt{2}\right)(\sin\theta)^2 + \frac{1}{3}(\sin\theta)^3\right) a^2 p \qquad \text{for } y \in [0; \tfrac{\sqrt{2}}{2}a] \qquad (26)$$

p_R, $m_{r,R}$ and $m_{r\theta,R}$ are again determined by:

$$p_R = v_x \cdot \cos\theta + v_y \cdot \sin\theta \qquad (27)$$

$$m_{r,R} = m_x \cos^2\theta + m_y \sin^2\theta \qquad (28)$$

$$m_{r\theta,R} = m_x \cos\theta \sin\theta - m_y \sin\theta \cos\theta \qquad (29)$$

p_R, $m_{r,R}$ og $m_{r\theta,R}$ are sketched for $\theta \in [0; 45^\circ]$ in figure 9.

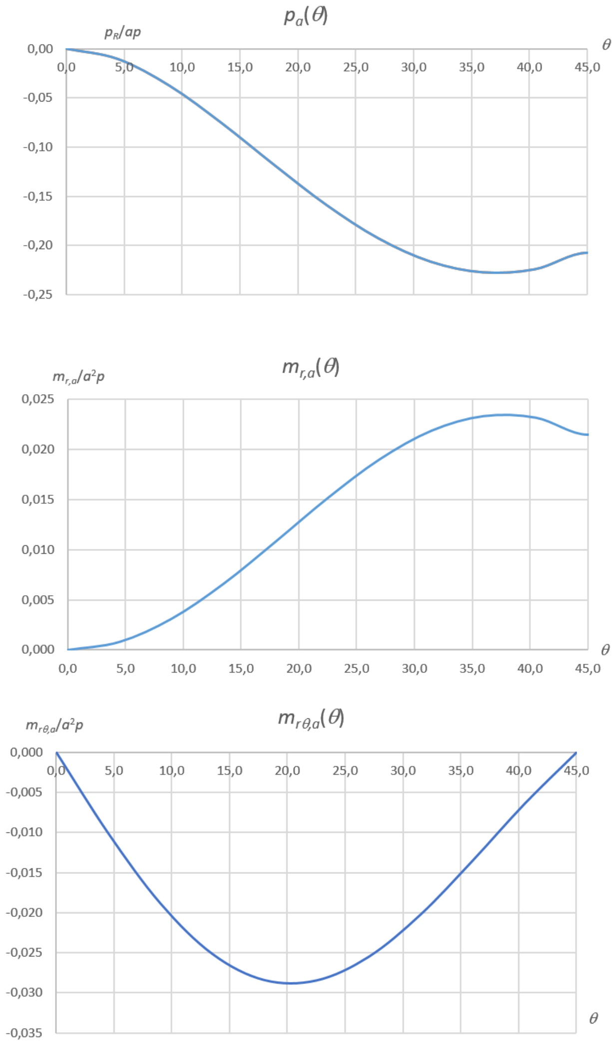

Figure 9 Model 3. $p_R(\theta)$, $m_R(\theta)$ and $m_{r\theta,R}$

Assessment of the models

By comparing the curves in Figures 5, 7 and 9, it can be seen that the most homogeneous, evenly distributed section force curves are obtained with model 3. Therefore, this model is applied.

Mean values:

$$\overline{p_{r,a}} = \frac{1}{a \cdot \frac{\pi}{4}} \int_0^{\frac{\pi}{4}} p_{r,a} \cdot a \cdot d\theta = -\left(\frac{1}{2} - \frac{2}{\pi}\right) ap \tag{40}$$

$$\overline{m_{r,a}} = \frac{1}{a \cdot \frac{\pi}{4}} \int_0^{\frac{\pi}{4}} m_{r,a} \cdot a \cdot d\theta \approx 0{,}013 \cdot a^2 p \tag{41}$$

$$\overline{m_{r\theta,a}} = \frac{1}{a \cdot \frac{\pi}{4}} \int_0^{\frac{\pi}{4}} m_{r\theta,a} \cdot a \cdot d\theta = -0{,}0178 \cdot a^2 p \tag{42}$$

The approximate expressions used are given by:

$$p_{r,a} \approx \overline{p_{r,a}} - \overline{p_{r,a}} \cdot \cos(4\theta) \tag{43}$$

$$m_{r,a} \approx -\overline{m_{r,a}} + \overline{m_{r,a}} \cdot \cos(4\theta) \tag{44}$$

$$m_{r\theta,a} \approx -\frac{\pi}{2} \cdot \overline{m_{r\theta,a}} \cdot \sin(4\theta) \tag{45}$$

These expressions give the same resultant reaction/moment as those modeled under model 3.

In figure 10, the approximate expressions are seen together with the calculated expressions.

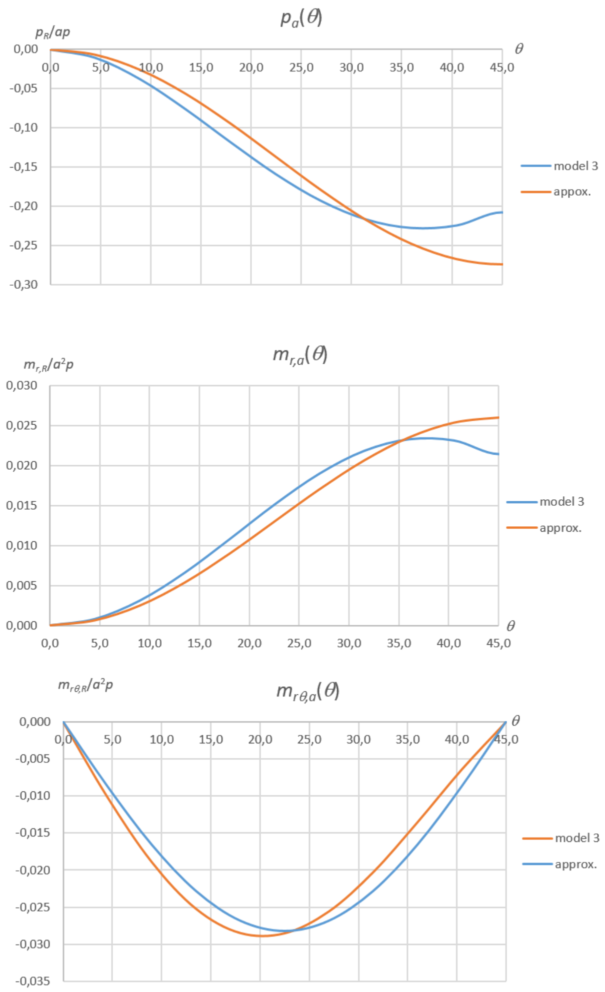

Figure 10 Approximate expressions sketched together with model 3

Section forces in foundations

The part of the reaction located within the circumscribed circle causes moments according to formulas (1) and (2). In the following, expressions for the section forces within the circumscribed circle are set up from the part of the reaction which is located outside the circumscribed circle. The section forces from this part, located outside the circumscribed circle, are given by the expressions shown in the formulas (43) - (45).

The amplitudes of the approximate expressions are determined so that the resulting response and the resulting moments are identical to the calculated expressions.

Only the part of the section forces that must necessarily go to the center of the foundation is taken to the center. The only section force that must necessarily be carried to the center is the mean value of the line load on the edge. The other section forces, m_r and $m_{r\theta}$, on the edge of the inscribed circle acting on the edge are balanced by section forces on the outermost part of the inscribed ring. It has been *chosen* to use a ring for this purpose, applicable for $r \in [\frac{3}{5}a; a]$.

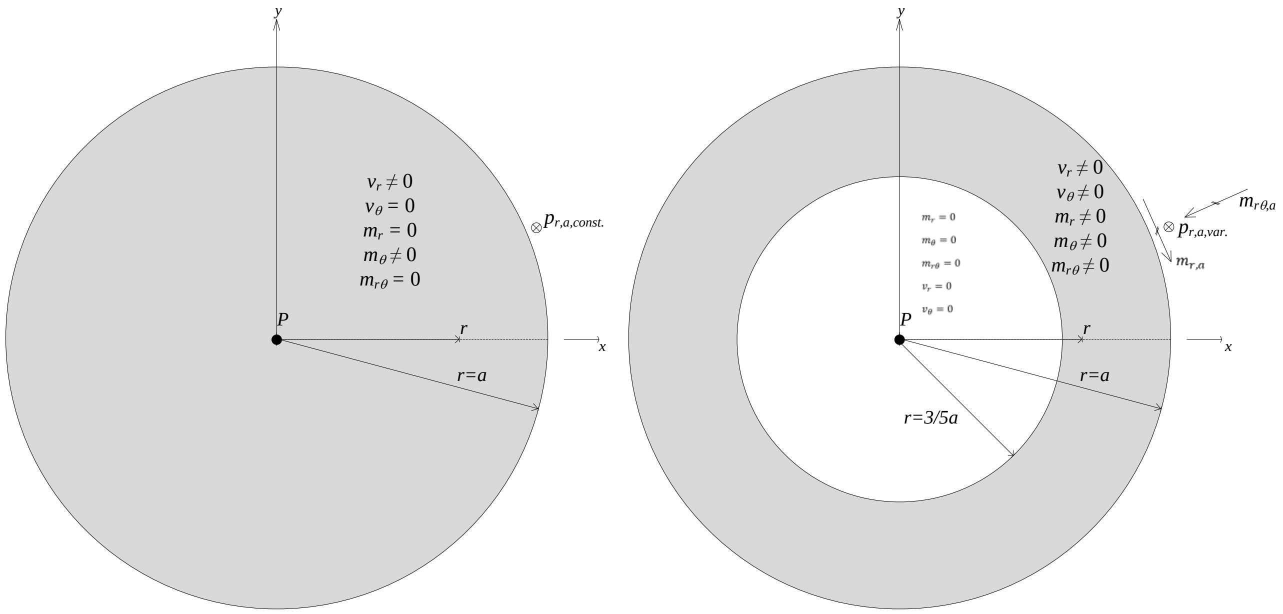

Figure 11 Modelling of sections forces acting at the edge of the circle

Line load on the edge

The line load on the edge of the inscribed circle is expressed by (43). In (46) an expression is given that satisfies this boundary condition and gives a simple, admissible variation as a function of r.

For $r \in [0; \frac{3}{5}a]$

$$v_r = \left(\frac{2}{\pi} - \frac{1}{2}\right) \cdot \left(-\frac{\mathrm{a}}{\mathrm{r}}\right) \cdot ap \tag{46}$$

The following section forces satisfy the equilibrium equations, just as they satisfy the boundary conditions.

$$v_\theta = 0 \tag{47}$$

$$m_r = 0 \tag{48}$$

$$m_\theta = \left(\frac{2}{\pi} - \frac{1}{2}\right) \cdot a^2 p \tag{49}$$

$$m_{r\theta} = 0 \tag{50}$$

For $r \in [\frac{3}{5}a; a]$

The line load on the edge of the inscribed circle is expressed by (43). In (46) an expression is given that satisfies this boundary condition and gives a simple, admissible variation as a function of *r*.

$$v_r = \left(\frac{2}{\pi} - \frac{1}{2}\right) \cdot \left(-\frac{\mathrm{a}}{\mathrm{r}} + \frac{5}{2} \cdot \left(\frac{r}{a} - \frac{3}{5}\right) \cdot \cos(4\theta)\right) \cdot ap \quad (51)$$

The following section forces satisfy the equilibrium equations, just as they satisfy the boundary conditions.

$$v_\theta = -\left(\frac{2}{\pi} - \frac{1}{2}\right) \cdot \left(\frac{5}{4}\frac{r}{a} - \frac{3}{5}\right) \cdot \sin(4\theta) \cdot ap \quad (52)$$

$$m_\theta = \left(\frac{2}{\pi} - \frac{1}{2}\right)\left(1 + \frac{1}{128}\left(55475\left(\frac{r}{a}\right)^3 - 71440\left(\frac{r}{a}\right)^2 + 21591\left(\frac{r}{a}\right) - 1248\right) \cdot \left(\frac{r}{a} - \frac{3}{5}\right) \cdot \left(\frac{r}{a} - 1\right) \cdot \cos(4\theta)\right) \cdot a^2 p \quad (53)$$

$$m_r = -\left(\frac{2}{\pi} - \frac{1}{2}\right) \cdot \frac{1}{256}\left(23775\left(\frac{r}{a}\right)^3 - 68760\left(\frac{r}{a}\right)^2 + 61817\left(\frac{r}{a}\right) - 17472\right) \cdot \left(\frac{r}{a} - \frac{3}{5}\right) \cdot \left(\frac{r}{a} - 1\right) \cdot \cos(4\theta) \cdot a^2 p \quad (54)$$

$$m_{r\theta} = -\left(\frac{2}{\pi} - \frac{1}{2}\right) \cdot \frac{1}{32}\left(7925\left(\frac{r}{a}\right)^3 - 14020\left(\frac{r}{a}\right)^2 + 6649\left(\frac{r}{a}\right) - 624\right) \cdot \left(\frac{r}{a} - \frac{3}{5}\right) \cdot \left(\frac{r}{a} - 1\right) \cdot \sin(4\theta) \cdot a^2 p \quad (55)$$

Bending moment on the edge for $r \in [\frac{3}{5}a; a]$

The bending moment on the edge of the inscribed circle is expressed by (44). In (56) an expression is given that satisfies this boundary condition and a boundary condition given by $m_r = 0$ for $r = 3/5a$ and gives a simple, permissible variation as a function of *r*.

The following section forces satisfy the equilibrium equations, just as they satisfy the boundary conditions. As supplementary boundary conditions, it has been chosen to require that $m_\theta = 0$ for $r = 3/5a$ and for $r = a$.

$$m_r = -0{,}013 \cdot \frac{5}{4}\left(-30\left(\frac{r}{a}\right)^2 + 53\frac{r}{a} - 21\right)\left(\frac{3}{5} - \frac{r}{a}\right)(1 - \cos(4\theta)) \cdot a^2 p \quad (56)$$

$$v_r = -0{,}013 \cdot \frac{1}{2}\left(-160 + 28 \cdot \frac{a}{r}\right) \cdot \left(\frac{3}{5} - \frac{r}{a}\right) \cdot \left(1 - \frac{r}{a}\right) \cdot \cos(4\theta) \cdot ap \quad (57)$$

$$v_\theta = -0{,}013 \cdot \frac{1}{10} \cdot \left(600\left(\frac{r}{a}\right)^2 - 710\left(\frac{r}{a}\right) + 176\right) \cdot \sin(4\theta) \cdot ap \quad (58)$$

$$m_\theta = -0{,}013 \cdot \frac{5}{4} \cdot \left(120\frac{r}{a} - 21\right)\left(\frac{3}{5} - \frac{r}{a}\right) \cdot \left(1 - \frac{r}{a}\right) \cdot \left(1 + \frac{1}{15} \cdot \cos(4\theta)\right) \cdot a^2 p \quad (59)$$

$$m_{r\theta} = -0{,}013 \cdot \frac{1}{2} \cdot \left(-40 \cdot \frac{r}{a} + 7\right) \cdot \left(\frac{3}{5} - \frac{r}{a}\right) \cdot \left(1 - \frac{r}{a}\right) \cdot \sin(4\theta)\, a^2 p \quad (60)$$

The twisting moment on the edge for $r \in [\frac{3}{5}a; a]$

The twisting moment on the edge of the inscribed circle is expressed by (45). In (61) an expression is given that satisfies this boundary condition as well as a boundary condition given by $m_r = 0$ for $r = 3/5a$ and gives a simple, permissible variation as a function of *r*.

$$m_{r\theta} = -\frac{\pi}{2} \cdot 0{,}0178 \cdot \frac{1}{72}\left(\frac{r}{a} - \frac{3}{5}\right) \cdot \left(-11\left(\frac{r}{a}\right)^2 + 431\frac{r}{a} - 240\right) \cdot \sin(4\theta) \cdot a^2 p \quad (61)$$

By only considering the twisting moment, it follows that the other section forces on the edge, v_r and m_r must be 0. The following expressions for v_r, v_θ, m_r and m_θ together with (61) satisfy the equilibrium equations and the boundary conditions:

$$v_r = -\frac{\pi}{2} \cdot 0{,}0178 \cdot \frac{1}{18}\left(\frac{r}{a} - 1\right)\left(\frac{r}{a} - \frac{3}{5}\right)\left(3200\frac{r}{a} - 1981\right) \cdot \cos(4\theta) \cdot ap \quad (62)$$

$$v_\theta = -\frac{\pi}{2} \cdot 0{,}0178 \cdot \frac{1}{360}\left(-64000\left(\frac{r}{a}\right)^3 + 106515\left(\frac{r}{a}\right)^2 - 50896\frac{r}{a} + 5943\right) \cdot \sin(4\theta) \cdot ap \quad (63)$$

$$m_r = -\frac{\pi}{2} \cdot 0{,}0178 \cdot \frac{1}{9} \cdot \left(\frac{r}{a} - 1\right)\left(\frac{r}{a} - \frac{3}{5}\right)\left(400\left(\frac{r}{a}\right)^2 - 415\frac{r}{a} + 105\right) \cdot \cos(4\theta) \cdot a^2 p \quad (64)$$

$$m_\theta = -\frac{\pi}{2} \cdot 0{,}0178 \cdot \frac{1}{9} \cdot \left(\frac{r}{a} - 1\right)\left(\frac{r}{a} - \frac{3}{5}\right)\left(400\left(\frac{r}{a}\right)^2 - 24\frac{r}{a} - 15\right) \cdot \cos(4\theta) \cdot a^2 p \quad (65)$$

In general, the section forces and moments can be expressed in terms of *x* and *y* by the following relations:

$$\theta = \operatorname{atan}\left(\frac{y}{x}\right) \quad (66)$$

$$r = \sqrt{x^2 + y^2} \quad (67)$$

Figure 12 shows m_θ (mq), m_r (mr) and $m_{r\theta}$ (mrq) for 0, 22.5 and 45 degrees respectively.

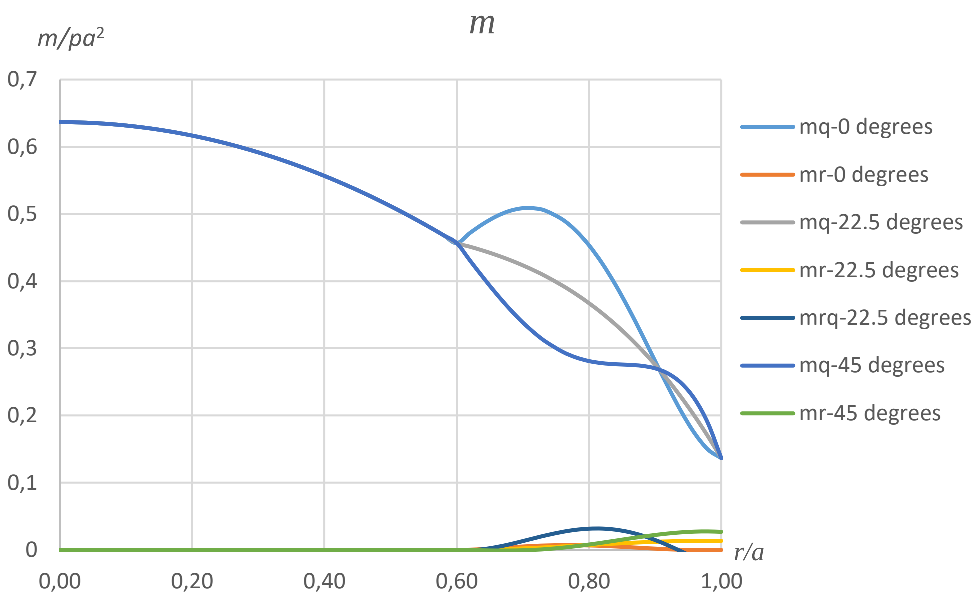

Figure 12 m_θ, m_r and $m_{r\theta}$. Concentrated load acting in a single point

It can be seen from the graphs that m_θ is totally dominant. Also for $r \in [\frac{3}{5}a; a]$ the variation and values for m_θ are seen to be significantly greater than the variation and values for both m_r and $m_{r\theta}$.

Figure 13 shows v_θ (vq) and v_r (vr) for 0, 22.5 and 45 degrees respectively.

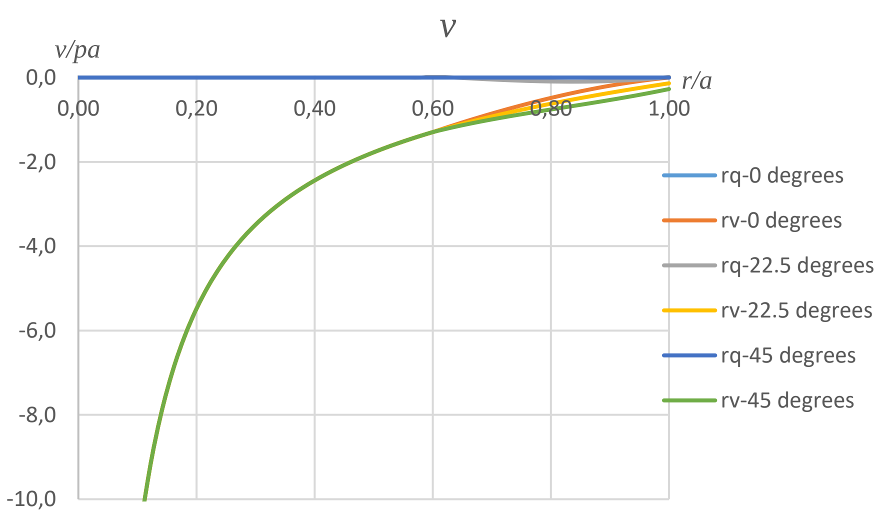

Figure 13 Figure 12 v_θ and v_r. Concentrated load acting in a single point

It can be seen from the graphs that v_r is totally dominant.

Section forces in square foundations affected by a load over a finite area

By considering a foundation affected by a load acting over a finite area rather than a concentrated point load, this can be done by simply changing the distribution of the section forces for the part of the reaction that is absorbed within the inscribed circle. This only means that the formulas (1) and (3) must be modified. The approach is therefore completely identical to the modification of the circular foundation.

As for the circular foundation, there is an area of m_θ with a constant value. The magnitude of this constant moment is determined by the deduction from the moment in a section through the center corresponding to the moment from ½$P \cdot e_2$, see figure 14. This deduction is expressed by a distance R in which the moment of the parabolic expression for m_θ exactly corresponds to this moment.

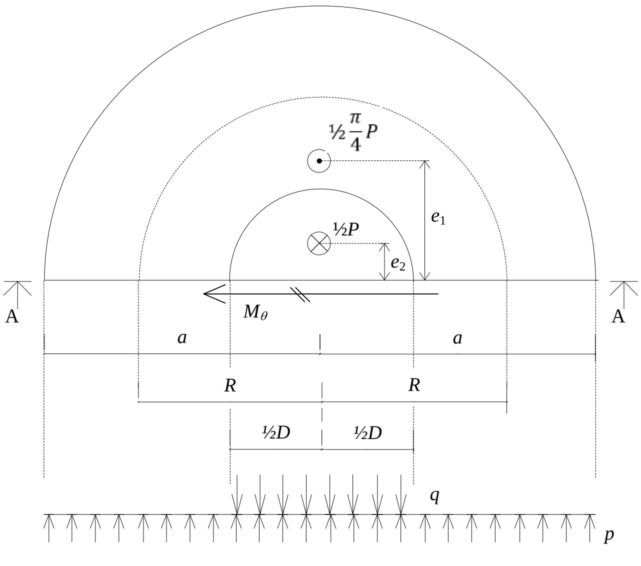

Figure 14 Section through the center of the circular foundations

$$\frac{1}{2}P \cdot e_2 = 2R \cdot \frac{2}{3} \cdot \left(\frac{1}{2}\left(\frac{R}{a}\right)^2 a^2 \cdot p\right) \tag{68}$$

$$\frac{1}{2}P \cdot \frac{4 \cdot \frac{1}{2}D}{3 \cdot \pi} = 2R \cdot \frac{2}{3} \cdot \left(\frac{1}{2}\left(\frac{R}{a}\right)^2 a^2 \cdot \frac{P}{(2a)^2}\right) \tag{69}$$

$$R = \sqrt[3]{\frac{2Da^2}{\pi}} \tag{70}$$

The constant value of m_θ is thus given by:

$$m_{\theta,1} = \frac{1}{2}\left(1 - \left(\frac{r}{a}\right)^2\right) a^2 \cdot p \tag{71}$$

$$m_{\theta,1} = \frac{1}{2}\left(1 - \left(\frac{\sqrt[3]{\frac{2Da^2}{\pi}}}{a}\right)^2\right) a^2 \cdot \frac{P}{4 \cdot a^2} \tag{72}$$

$$m_{\theta,1} = \frac{1}{8}\left(1 - \left(\sqrt[3]{\frac{2D}{\pi a}}\right)^2\right) P \tag{73}$$

This is valid for $r < R$.

Thereby:

$$m_\theta = \frac{1}{8}\left(1-\left(\sqrt[3]{\frac{2D}{\pi a}}\right)^2\right)P \quad \text{for } r \in [0;R] \tag{74}$$

$$m_\theta = \frac{1}{8}\left(1-\left(\frac{r}{a}\right)^2\right)P \quad \text{for } r \in [R;a] \tag{75}$$

$$m_r = \frac{P}{8}\left(\frac{1}{3}\left(\frac{1}{a^2}-\frac{4}{\pi}\frac{4}{D^2}\right)r^2+\frac{4}{\pi}-\left(\sqrt[3]{\frac{2\cdot D}{\pi\cdot a}}\right)^2\right) \quad \text{for } r \in [0;½D] \tag{76}$$

$$m_r = \frac{P}{8}\left(\frac{1}{3}\left(\frac{r}{a}\right)^2-\left(\sqrt[3]{\frac{2\cdot D}{\pi\cdot a}}\right)^2-\left(\frac{1}{3}\left(\frac{R}{a}\right)^2-\left(\sqrt[3]{\frac{2\cdot D}{\pi\cdot a}}\right)^2\right)\frac{R}{r}\right) \quad \text{for } r \in [½D;R] \tag{77}$$

$$m_r(r) = 0 \quad \text{for } r \in [R;a] \tag{78}$$

$$v_r = -\frac{P}{8r}\left(1-\left(\frac{r}{a}\right)^2\right)+\frac{P}{2\pi r}\left(1-4\left(\frac{r}{D}\right)^2\right) \quad \text{for } r \in [0;½D] \tag{79}$$

$$v_r = -\frac{P}{8r}\left(1-\left(\frac{r}{a}\right)^2\right) \quad \text{for } r \in [½D;a] \tag{80}$$

For the line load applies to $r \in [0;½D]$

$$m_\theta = \frac{\left(\frac{2}{\pi}-\frac{1}{2}\right)}{\left(\frac{1}{2}D\right)^2}r^2\cdot pa^2 \tag{81}$$

$$m_r = 0 \tag{82}$$

$$m_{r\theta} = 0 \tag{83}$$

$$v_\theta = 0 \tag{84}$$

$$v_r = -\frac{\left(\frac{2}{\pi}-\frac{1}{2}\right)}{\left(\frac{1}{2}D\right)^2}r\cdot pa \tag{85}$$

For $r > ½D$ the sectional forces from the line load on the edge are unchanged, i.e. (46)-(55).

Residual stresses for $r \in [\frac{3}{5}a;a]$

The "band" of section forces for $r \in [\frac{3}{5}a;a]$ means, in the event that the extent of the column is taken into account, that m_θ can have a value greater than the constant moment at the center of the foundation. In order for this not to be dimensional, a residual stress state is set up below that reduces the monent at the critical locations. The constants in the expressions are adapted below so that m_θ has a maximum value in the band for $r \in [\frac{3}{5}a;a]$ which is identical to the constant moment at the center for the case $D/a = 0.24$.

$$v_r = \frac{1}{6}\left(\frac{r}{a}-1\right)\left(\frac{r}{a}-\frac{3}{5}\right)\left(32\frac{r}{a}-21\right)\cdot\cos(4\theta)\cdot ap \tag{86}$$

$$v_\theta = \frac{1}{120}\left(-640\left(\frac{r}{a}\right)^3+1083\left(\frac{r}{a}\right)^2-528\frac{r}{a}+63\right)\cdot\sin(4\theta)\cdot ap \tag{87}$$

$$m_\theta = \frac{1}{480}\left(\frac{r}{a}-\frac{3}{5}\right)\left(925\left(\frac{r}{a}\right)^3-893\left(\frac{r}{a}\right)^2+33\frac{r}{a}+27\right)\cdot\cos(4\theta)\cdot a^2p \tag{88}$$

$$m_r = \frac{1}{480}\cdot\left(\frac{r}{a}-1\right)\left(\frac{r}{a}-\frac{3}{5}\right)\left(545\left(\frac{r}{a}\right)^2-642\frac{r}{a}+189\right)\cdot\cos(4\theta)\cdot a^2p \tag{89}$$

$$m_{r\theta} = \frac{1}{480}\left(\frac{r}{a}-1\right)\left(\frac{r}{a}-\frac{3}{5}\right)\cdot\left(-190\left(\frac{r}{a}\right)^2-12\frac{r}{a}+54\right)\cdot\sin(4\theta)\cdot a^2p \tag{90}$$

Figure 15 shows m_θ (mq), m_r (mr) and $m_{r\theta}$ (mrq) for 0, 22.5 and 45 degrees respectively. When calculating the graphs, $D/a = 0.24$ is applied.

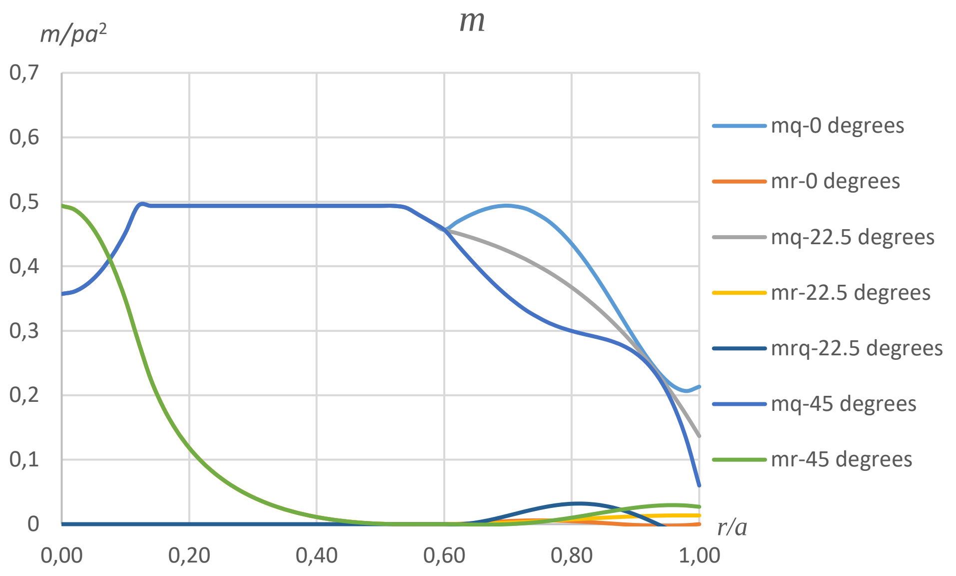

Figure 15 Figure 12 m_θ, m_r and $m_{r\theta}$. Concentrated load acting over a finite area

It can be seen from the graphs that m_θ is again totally dominant. For $r \to 0$ it is seen that m_r have an increasing value with a value for $r = 0$ corresponding to the maximum value for m_θ. Also for $r \in [\frac{3}{5}a; a]$ the variation and values for m_θ are seen to be significantly greater than the variation and values for both m_r and $m_{r\theta}$.

Figure 16 shows v_θ (vq) and v_r (vr) for 0, 22.5 and 45 degrees respectively.

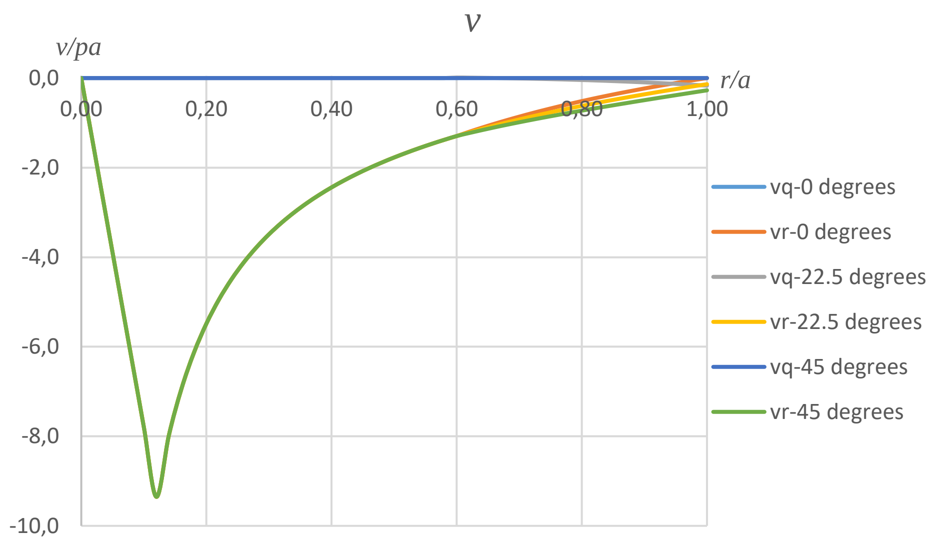

Figure 16 v_θ and v_r. Concentrated load acting over a finite area

As was the case for $D/a = 0$, it can be seen from the graphs that v_r is totally dominant.

Principal moments

m_x, m_y and m_{xy} is determined by formulas (B.5)-(B.7). Based on these, the main moments can be determined by:

$$\begin{matrix} m_1 \\ m_2 \end{matrix} = \frac{m_x+m_y}{2} \pm \sqrt{\left(\frac{m_x-m_y}{2}\right)^2 + m_{xy}^2} \tag{91}$$

The maximum value of m_1 is found in the center of the foundation and is given by:

$$m_{1,max} = \frac{2}{\pi} a^2 p \tag{92}$$

This value in the center can be directly seen from the formulas (3) and (49), since the only quantities that give a value different from 0 in the center are $m_{\theta,c}$ and $m_{\theta,p}$.

For the circular foundation affected by a point load, $m_2 = 0$ throughout the foundation. For the square foundation, there are non-negative moments with a moment at the center of $m_2 = 0$ with slightly increasing values towards the edge of the inscribed circle and with a maximum value for $r = a$ and $\theta = 45^o$ with a value of $m_2 = 0{,}027a^2p$ (approx. 4% of the maximum value of m_1).

Figure 17 shows $m_1(r/a)$ for $\theta = 0$ degrees and $\theta = 45$ degrees, respectively. In this case the residual stresses are not included.

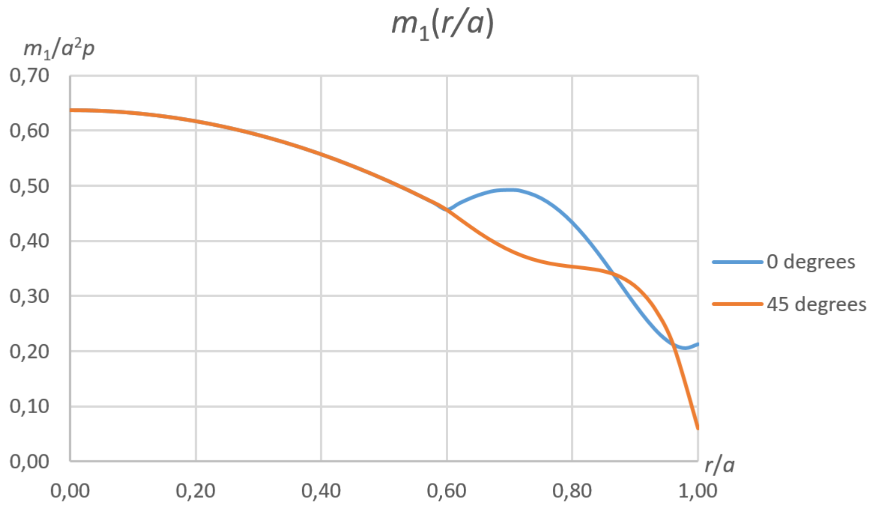

Figure 17 m_1. Concentrated load acting in a single point

Figure 18 shows the same for the case where the extent of the column is taken into account with $D/a = 0.24$. The residual stresses given by formulas (86) - (90) are included.

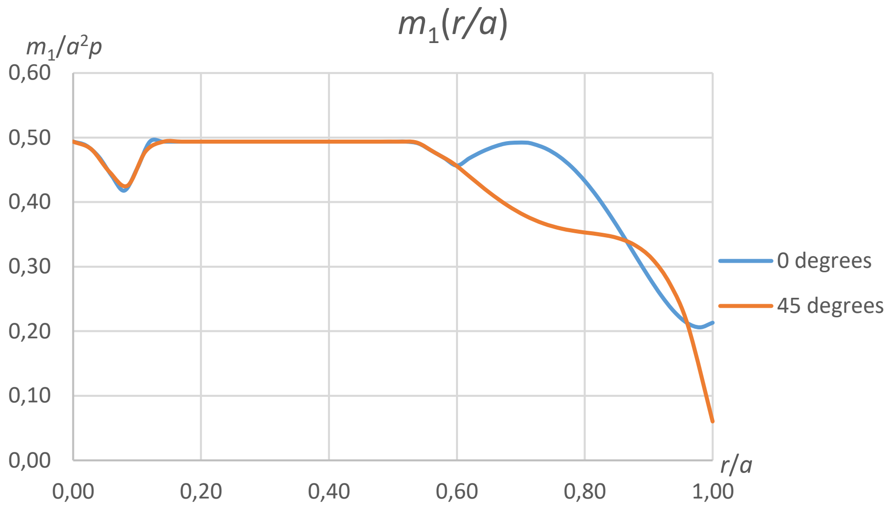

Figure 18 m_1. Concentrated load acting over a finite area

Comparison between the circular foundation and the square foundation

The maximum moment in the circular foundation expressed by the column reaction *P*:

$$m_{max} = \frac{P}{2\pi} \quad (93)$$

Correspondingly, the maximum moment in the square foundation is expressed by the column reaction *P*.

$$m_{1,max} = \frac{2}{\pi} a^2 p \quad (94)$$

With $P = (2a)^2 p$ inserted:

$$m_{max} = \frac{P}{2\pi} \quad (95)$$

It is thus seen that the design moment is the same for a circular moment and a square foundation, affected by the same normal force, provided that the area of the two foundations is the same. The same area means that the ratio between the radius of the circular foundation, *R*, and the half side length of the square foundation, *a*, is given by:

$$\frac{R}{a} = \sqrt{\frac{4}{\pi}} \quad (96)$$

An analogy is obtained for the relationship between the maximum moment for circular and square foundations, respectively, for columns of finite extent.

Examination of anchorage

Assuming no anchored/bent reinforcement is used at the edge of the point foundation, the moment capacity decreases towards the edge. Since the anchorage is assumed to vary linearly, it is assumed correspondingly that the moment capacity decreases linearly at a distance from the edge corresponding to the anchorage length in both directions.

This is illustrated in figure 19. A point C is considered, which lies at a distance from the edge which is less than the anchoring length. Since the distance from the edge is different in the two directions, this also means that the moment capacity at this point is different in the two directions.

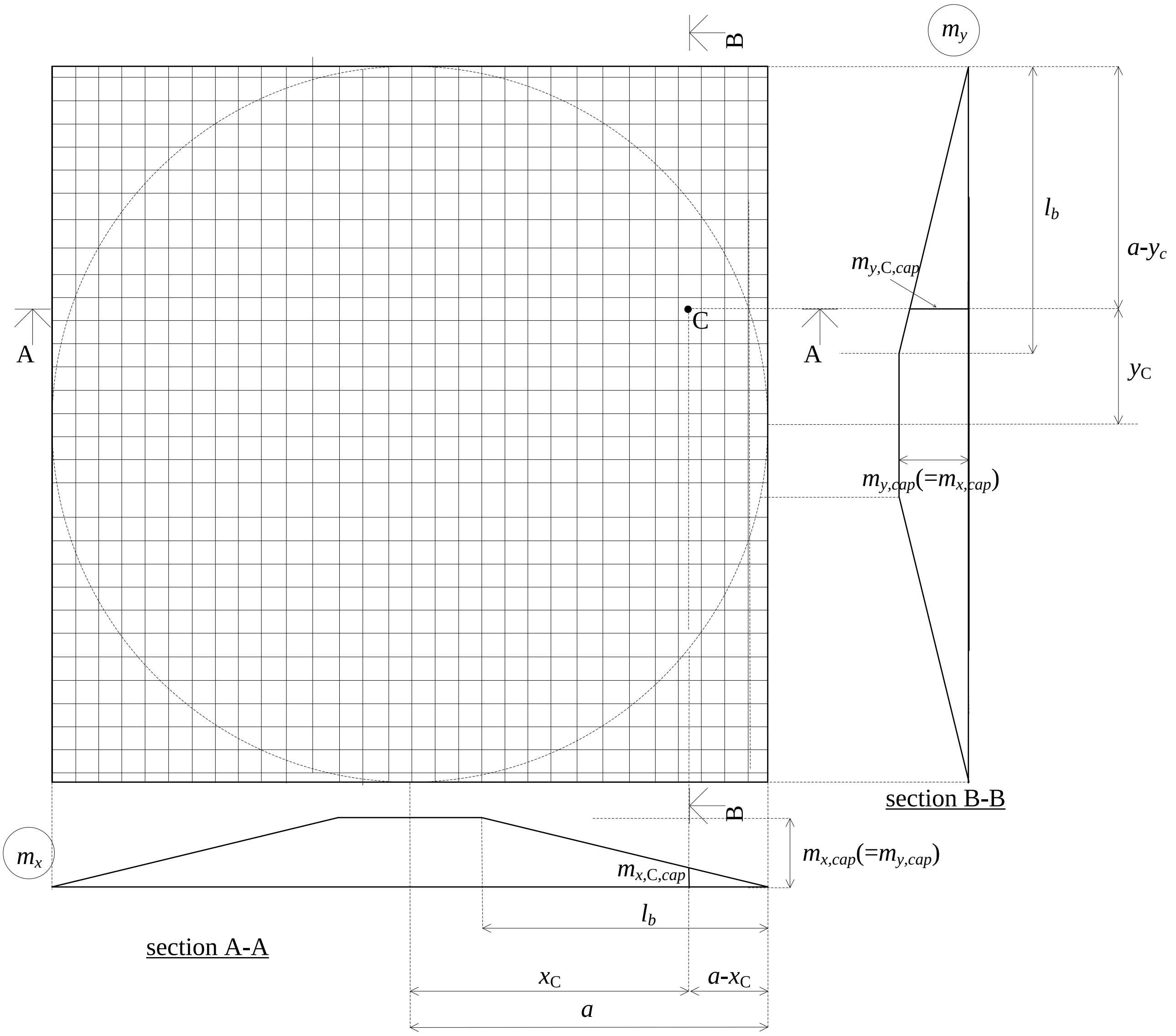

Figure 19 Square foundation with orthogonal reinforcement and decreasing moment capacity towards the edge

The optimal utilization of the reinforcement in a zone closer than the anchorage length from the edge is achieved by taking into account the varying moment capacity. The ratio between the moment capacities in the two directions can be expressed by the inverse of the ratio between the distances to the edge in the two directions:

$$m_{sy} = \frac{a-y}{a-x} m_{sx} \quad (97)$$

With the expressions for m_{sx} and m_{sy} inserted:

$$m_y + \chi|m_{xy}| = \frac{a-y}{a-x} m_x + \frac{a-y}{a-x} \cdot \frac{1}{\chi}|m_{xy}| \quad (98)$$

From this expression, χ can be determined:

$$0 = \chi^2|m_{xy}| + \left(m_y - \frac{a-y}{a-x} m_x\right) \cdot \chi - \frac{a-y}{a-x} \cdot |m_{xy}| \quad (99)$$

$$0 = \chi^2 + \frac{\left(m_y - \frac{a-y}{a-x} \cdot m_x\right)}{|m_{xy}|} \cdot \chi - \frac{a-y}{a-x} \quad (100)$$

Which gives:

$$\chi = -\frac{1}{2}\frac{\left(m_y - \frac{a-y}{a-x}\cdot m_x\right)}{|m_{xy}|} + \frac{1}{2}\sqrt{\frac{\left(m_y - \frac{a-y}{a-x}m_x\right)^2}{m_{xy}^2} + 4\cdot\frac{a-y}{a-x}} \quad (101)$$

That is, with this value of χ, m_{sx} and m_{sy} can be determined. Thus, although the point foundation is isotropically reinforced, it behaves at the edge as anisotropically reinforced with a linearly decreasing moment capacity towards the edge in each of the two directions.

In addition, there are the two cases where only the reinforcement in one direction is fully anchored, while the reinforcement in the other direction is not fully anchored:

$$\frac{a-y}{l_b} \text{ for } a-y > l_{b,max} \wedge a-x \leq l_{b,max} \quad (102)$$

$$\frac{l_b}{a-x} \text{ for } a-y \leq l_{b,max} \wedge a-x > l_{b,max} \quad (103)$$

With the assumption that $T_{sx}/(P/2\pi z)$ this is seen in figure 20 for different values of y/a the linearly decreasing strong line that has a slope corresponding to reaching the maximum value at a distance of $0.7\cdot a$ from the edge . This is analogous to what was found for the circular foundation.

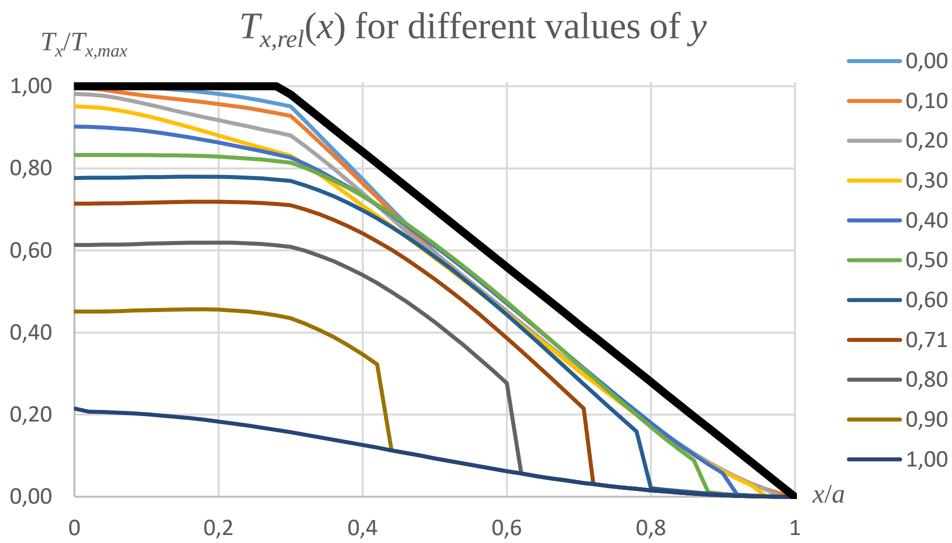

Figure 20 $T_{sx}/(P/2\pi z)$ for different values of y/a. Concentrated load acting in a single point

Figure 21 shows the equivalent for a square foundation affected by a load acting over a finite area. In figure 21 this is shown for a ratio of D/a = 0.24. By taking into account the extent of the load, the maximum value is reached at a distance of $0.5\cdot a$ from the edge. This means that the maximum anchorage length to avoid bent reinforcement in a square foundation with $D/a \leq 0.24$ is $l_{b,max} = 0.5\cdot a$.

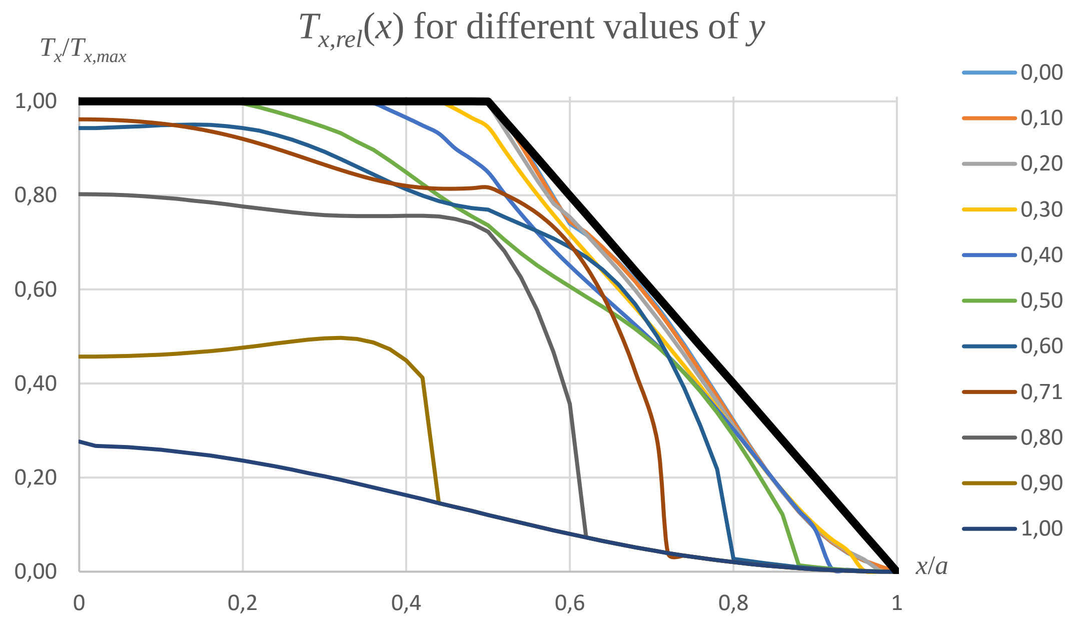

Figure 21 $T_{sx}/(P/2\pi z)$ for different values of y/a. Concentrated load acting over a finite area

Conclusion

This study analyzed a square foundation subjected to a centrally located point load, followed by an examination of the foundation under a distributed load. The foundation was reinforced with orthogonal, isotropic reinforcement at the bottom, and the problem was approached using the lower bound theorem to determine the section forces across the entire foundation. The primary goal was to compare these results with similar analyses of a circular foundation, also reinforced in the same manner and subjected to a centrally located point load.

The modeling of the square foundation was informed by the analysis of the circular foundation. Within the inscribed circle, the stress distribution for the reaction inside this circle was found to be identical to that in the circular foundation. For the reaction outside the inscribed circle, three different approaches were considered for transferring this force to the edge of the circle. The approach (model 3) that produced the smallest variation at the edge was selected for further analysis. The stress distributions were then developed within the inscribed circle for the reaction located outside it. Here, the reaction at the edge of the inscribed circle was directed towards the center of the foundation, while the bending and twisting moments at the edge were considered along the outer boundary of the inscribed circle. A band thickness of $2/5 \cdot a$ was used in this treatment, and it was demonstrated that these stress distributions satisfied equilibrium conditions. Additionally, a residual stress state was applied within this region of the inscribed circle.

The results show that the moment capacity of the square foundation is identical to that of the circular foundation, provided both have the same area. The variation in the force within the reinforcement also mirrors that of the circular foundation, decreasing towards the edge in a similar manner. It was found that m_θ and v_r govern the design for both foundation types. m_r matches m_θ at the center of the foundation when the column's extent is considered, but decreases sharply at a short distance from the center. The magnitudes of the other section forces were found to be very limited.

Regarding the maximum anchorage length to prevent application of bent-up reinforcement, the analysis revealed that for a point load the maximum anchorage length must fulfill $l_{b,max} = 0.7 \cdot a$. For a square foundation with $D/a \leq 0.24$, the maximum anchorage length is $l_{b,max} = 0.5 \cdot a$.

Literature

[1] Lars German Hagsten: ”Point Foundation. Lower Bound Solution for Distributed Load”. Proceedings of the Danish Society for Structural Science and Engineering. No. 1, May 2023, page 1-14.

[2] Lars German Hagsten: ” Required anchorage length of reinforcement in circular foundation subjec-ted by a centrally located normal force and supported by a uniformly distributed reaction”. Proceedings of the Danish Society for Structural Science and Engineering. No. 2, May 2023, page 1-12.

[3] M.P. Nielsen & L. C. Hoang: 'Limit Analysis and Concrete Plasticity'. Third edition. 2011. CRC Press

Appendix A. Equilibrium equations in polar coordinates

Equilibrium equations in polar coordinates according to figure A.1.

1. $v_r \cdot r = \frac{\partial(m_r \cdot r)}{\partial r} - \frac{\partial m_{r\theta}}{\partial \theta} - m_\theta$ (A.1)
2. $v_\theta \cdot r = \frac{\partial m_\theta}{\partial \theta} - \frac{\partial m_{r\theta}}{\partial r} r - 2m_{r\theta}$ (A.2)
3. $\frac{\partial(v_r \cdot r)}{\partial r} + \frac{\partial v_\theta}{\partial \theta} = -p \cdot r$ (A.3)

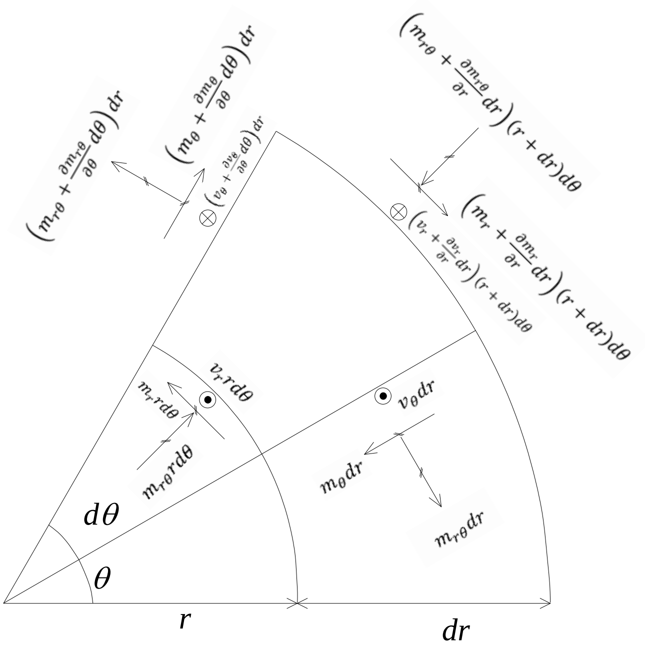

Figure A.1

Appendix B. Transformation formulas

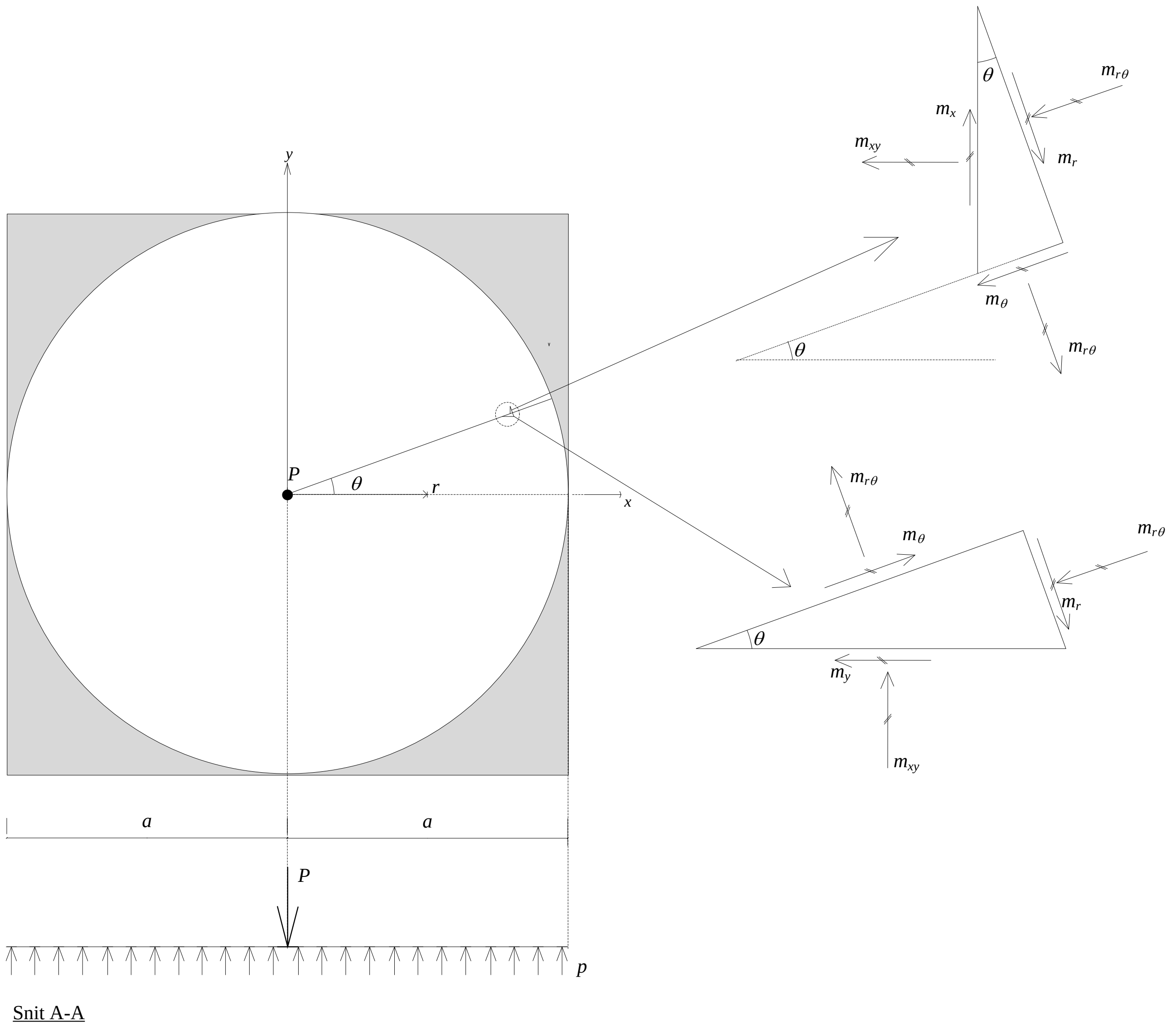

Figure B.1

$$m_x = m_r \cdot \cos^2\theta + m_\theta \cdot \sin^2\theta + 2m_{r\theta} \cdot \sin\theta \cdot \cos\theta \tag{B.1}$$

$$m_y = m_r \cdot \sin^2\theta + m_\theta \cdot \cos^2\theta - 2m_{r\theta} \cdot \sin\theta \cdot \cos\theta \tag{B.2}$$

$$m_{xy} = m_r \cdot \sin\theta \cdot \cos\theta - m_\theta \cdot \sin\theta \cdot \cos\theta + m_{r\theta}(\sin^2\theta - \cos^2\theta) \tag{B.3}$$

With

$$\theta = \arctan\left(\frac{y}{x}\right) \tag{B.4}$$

$$m_x = m_r \cdot \cos^2\left(\arctan\left(\frac{y}{x}\right)\right) + m_\theta \cdot \sin^2\left(\arctan\left(\frac{y}{x}\right)\right) + 2m_{r\theta} \cdot \sin\left(\arctan\left(\frac{y}{x}\right)\right) \cdot \cos\left(\arctan\left(\frac{y}{x}\right)\right) \tag{B.5}$$

$$m_y = m_r \cdot \sin^2\left(\arctan\left(\frac{y}{x}\right)\right) + m_\theta \cdot \cos^2\left(\arctan\left(\frac{y}{x}\right)\right) - 2m_{r\theta} \cdot \sin\left(\arctan\left(\frac{y}{x}\right)\right) \cdot \cos\left(\arctan\left(\frac{y}{x}\right)\right) \tag{B.6}$$

$$m_{xy} = (m_r - m_\theta) \cdot \sin\left(\arctan\left(\frac{y}{x}\right)\right) \cdot \cos\left(\arctan\left(\frac{y}{x}\right)\right) + m_{r\theta}\left(\sin^2\left(\arctan\left(\frac{y}{x}\right)\right) - \cos^2\left(\arctan\left(\frac{y}{x}\right)\right)\right) \tag{B.7}$$

Danish Society for Structural Science and Engineering

Requests for membership of the society are submitted to one of the board members:

Dennis Cornelius Pedersen, Chairman of the Board, Artelia

Andreas Bollerslev, Vice Chair, Niras

Jens Henrik Nielsen, Cashier, Cowi

Jesper Pihl, Board member, Cowi

Torben Bilgrav Bangsgaard, Board member , Rambøll

Simone Øst Grunnell, Board member, Niras

Henrik Stang, Board member, DTU

Henrik Maltha Kampmann, Board member, NCC

Frederik Jønsson Madsen, Student representative, DTU

Esther Bondensgård Boysen, Student representative, DTU

The purpose of the society is to work for the scientific development of structural mechanics - both theory and construction of all kinds of load-bearing structures - promote interest in the subject, work for a collegial relationship between its practitioners and assert its importance to and in collaboration with other branches of engineering. The purpose is sought realized through meetings with lectures and discussions as well as through the publication of the Proceedings of the Danish Society for Structural Science and Engineering.

Individual members, companies and institutions that are particularly interested in structural mechanics or whose company falls within the field of structural mechanics can be admitted as members.